

# Supporting information for Monoterpene oxidation pathways initiated by acyl peroxy radical addition

D. Pasik, T. Golin Almeida, E. Ahongshangbam, S. Iyer, and N. Myllys

## Addition of $\text{CH}_3\text{C}(\text{O})\text{OO}\cdot$ to double bond in $\alpha$ -pinene

The addition of  $\text{CH}_3\text{C}(\text{O})\text{OO}\cdot$  to  $\alpha$ -pinene was considered for both carbons in the double bond and for two different sides of radical attack. The investigated isomers, along with the calculated barriers for radical addition (green text), are presented in Figure S1. Significantly lower barrier is observed for the R-acetyl isomer, where the addition of the radical occurs from the opposite side of the methyl groups and the secondary ring. This phenomenon can be attributed to steric hindrance associated with addition from the same side as the ring and methyl groups.

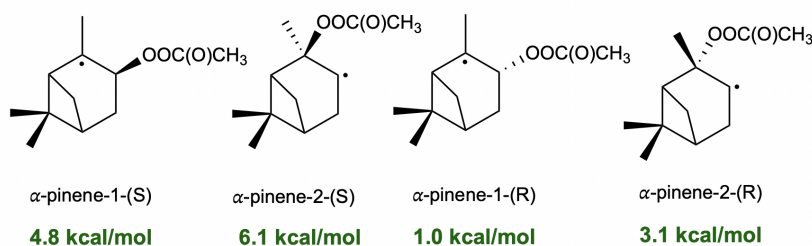


Figure S1: Four possible stereoisomers of  $\alpha$ -pinene + APR accretion product.

The addition of APR to  $\alpha$ -pinene through the formation of the R-stereoisomer and tertiary radical has the lowest barrier among the four positions, and the calculated MC-TST rate coefficient is  $3 \times 10^{-16} \text{ cm}^3\text{s}^{-1}$ . Based on the analysis conducted by Pasik et al. (2024a), the pseudo-first-order reaction rate coefficient will be  $4 \times 10^{-8} \text{ 1/s}$ , corresponding to up to 0.1% of  $\alpha$ -pinene OH-initiated oxidation. However, this value is associated with uncertainties, including the lack of experimentally measured rate constants for the APR + monoterpene reaction and the absence of new, precise measurements of APR concentrations in the atmosphere. Nevertheless, the authors emphasize the potential significance of APR-initiated reactions with unsaturated hydrocarbons and the need for further research in this area.

## Addition of $\text{CH}_3\text{C}(\text{O})\text{OO}\cdot$ to double bond in monoterpenes

For clarity, in the manuscript we present only the fastest APR accretion reactions to the monoterpenes. Table S1 presents the calculated energy barriers and rate coefficients for other APR + monoterpene reactions leading to secondary or tertiary alkyl radicals. Figure S2 shows the numbering.

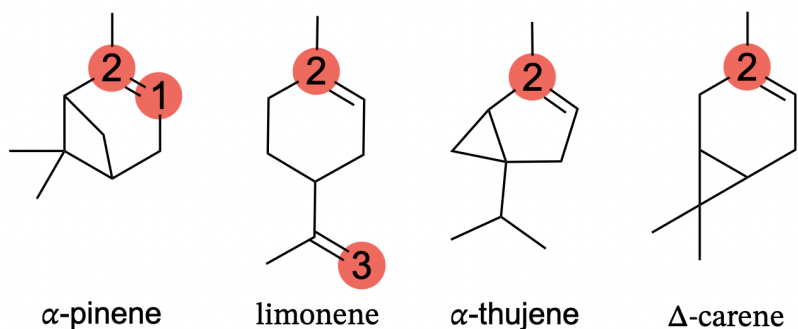


Figure S2: Structures of hydrocarbons undergoing the accretion reaction with APR. The considered addition positions are marked with colorful dots.

Table S1: Barrier heights and calculated MC-TST rates for accretion reaction between  $\text{CH}_3\text{C}(\text{O})\text{OO}\cdot$  and monoterpenes (less favourable positions). Labeling in the table refers to labeling on Figure S2. Barrier heights [kcal/mol] were calculated on DLPNO-CCSD(T)/aug-cc-pVTZ// $\omega$ B97X-D/6-31+G\*. Corresponding reaction rate coefficients for monoterpene + APR accretion reaction were calculated using MC-TST ( $k_{\text{MC-TST}}$ ) [ $\text{cm}^3 \text{s}^{-1}$ ]. Results for limonene and  $\alpha$ -pinene were adopted from Pasik et al. (2024a)

monoterpene	Barrier	$k_{\text{MC-TST}}$
limonene-2	4.2	$1 \times 10^{-18}$
limonene-3	2.8	$6 \times 10^{-18}$
$\alpha$ -pinene-1 (S)	4.8	$4 \times 10^{-19}$
$\alpha$ -pinene-2 (R)	3.1	$5 \times 10^{-18}$
$\Delta$ -carene-2	2.3	$6.7 \times 10^{-18}$
$\alpha$ -thujene-2 (R)	0.8	$1.0 \times 10^{-16}$
$\alpha$ -thujene-2 (S)	4.7	$9.9 \times 10^{-20}$

## Comparison of alkyl ring opening reaction rate coefficients using LC-TST and MESMER

As discussed in section 3.1 in main text, the rate coefficients derived from MESMER calculations are generally higher than those obtained using MC-TST. To address this, a comparative analysis was conducted between the rate coefficients derived from the single-conformer TST equation and those from MESMER (see LC-TST equation below).

$$k = \kappa_t \frac{k_{\text{BT}}}{h P_{\text{ref}}} \frac{Q_{\text{LTS}}}{Q_{\text{LR}}} \exp\left(-\frac{E_{\text{TS}} - E_{\text{R}}}{k_{\text{BT}}}\right) \quad (1)$$

where  $Q_{\text{LTS}}$  and  $Q_{\text{LR}}$  represent partition functions for lowest energy conformer of TS and reactants, respectively, the tunneling coefficient  $\kappa_t=1$  as the reaction is between heavy atoms. Obtained values were computed at the DLPNO-CCSD(T)/aug-cc-pVTZ// $\omega$ B97X-D/6-31+G\* level of theory.

The findings, as presented in Table S2, demonstrate that excess energy continues to drive the formation of ring-opened products, resulting in a significant discrepancy between the calculated reaction rate coefficients.

Table S2: Monoterpene-derived alkyl ring opening reaction rate coefficients calculated using lowest-conformer TST ( $k_{LC-TST}$ ) [ $\text{cm}^3 \text{s}^{-1}$ ] and their yield compared to RRKM-ME ( $\%_{RRKM}$ )

monoterpene	$k_{LC-TST}$	$\%_{TST}$	$\%_{RRKM}$
$\alpha$ -pinene	$1.8 \times 10^2$	$\sim 0$	$\sim 0$
$\beta$ -pinene	$5 \times 10^3$	$\sim 0$	2
camphene	$1 \times 10^{-4}$	$\sim 0$	$\sim 0$
sabinene	$5 \times 10^5$	11	39
$\alpha$ -thujene (R)	$9 \times 10^4$	2	20
$\alpha$ -thujene (S)	$2 \times 10^4$	$\sim 0$	12

### H-shift reactions for sabinene-derived peroxy radical

H-shift reactions for sabinene-derived peroxy radical were investigated (see Figure 14 Section 3.3.6 for overview). Table S3 shows calculated energy barrier heights and reaction rate coefficients for studied unimolecular reactions.

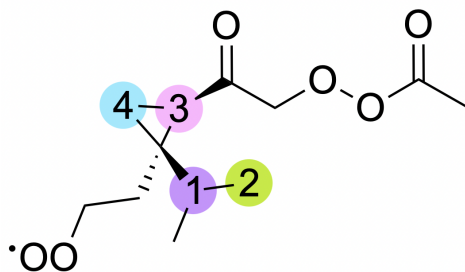


Figure S3: Labeling for H-shift reactions of sabinene-derived peroxy radical. The numbers on the scheme correspond to the numbering in the Table S3.

Table S3: Energy barrier heights [kcal/mol] and calculated MC-TST reaction rate coefficients [1/s] for studies H-shift reactions of sabinene-derived peroxy radical.

pathway	barrier	TST
H-shift-1	20.5	1.3E-01
H-shift-2	28.0	5.5E-03
H-shift-3	27.2	2.4E-07
H-shift-4	51.1	4.2E-20

### Optimization of grain size and $k_B T$ parameters for alkyl radical ring rearrangement calculations

For the alkyl radical ring rearrangement calculations performed using MESMER, we tested different grain sizes and spans of grains above the highest-energy transition state values using sabinene ring opening rearrangement as a test reaction. As shown by the data in Table S4, we observe an increase in the efficiency of the ring-opening reaction when increasing the  $k_B T$  parameter from 20 to 50. Moreover, further increasing the parameter (up to 75) does not lead to a rise in efficiency. Additionally, we do not observe any difference when changing the grain size while keeping the  $k_B T$  value constant. Therefore, in our calculations for all alkyl radical ring openings, we use a grain size of 30 and grains above the highest-energy transition state of 50.

Table S4: MESMER grain size spans of grains above the highest-energy transition state parameters comparison.

grain size	$k_B T$	yield [%]
30	20	30
30	50	39
50	20	30
50	50	39
30	75	39

### Lennard-Jones parameters for RRKM-ME calculations

Table S5: Lennard-Jones parameters  $\sigma$  and  $\epsilon$  used for the alkyl radical formed in reaction with APR (MT-APR), and the alkoxy radical formed from ring-opening rearrangement (ring-opened RO-APR) in RRKM-ME calculations.

monoterpene	MT-APR		ring-opened RO-APR	
	$\sigma$ (Å)	$\epsilon/k_B$ (K)	$\sigma$ (Å)	$\epsilon/k_B$ (K)
$\beta$ -pinene	7.72	593.35	7.69	584.29
$\alpha$ -pinene	7.74	585.00	7.95	613.50
sabinene	7.67	591.32	7.85	603.82
$\alpha$ -thujene	7.74	587.63	7.91	600.15
camphene (R1)	7.72	593.35	7.90	576.89
camphene (R2)	7.72	593.35	7.72	571.55
camphene (R3)	7.72	593.35	7.97	592.33

### References

D. Pasik, B. N. Frandsen, M. Meder, S. Iyer, T. Kurtén and N. Myllys, Gas-Phase Oxidation of Atmospherically Relevant Unsaturated Hydrocarbons by Acyl Peroxy Radicals, *Journal of the American Chemical Society*, 2024, 146, 13427–13437.